Kinetics of Fixed Bed Sorption Processes

Yasmen A. A. Mustafa

Department of Economics of Oil and Gas, University of Imam Jaafar Al-Sadiq, Baghdad, Iraq
yasmen.mustafa@gmail.com

ABSTRACT

Adsorption and ion exchange are examples of fixed-bed sorption processes that show transient behavior. This means that differential equations are needed to design them. As a result, numerical methods are commonly utilized to solve these equations. The solution frequently used in analytical methods is called the Thomas solution. Thomas gave a complete solution that adds a nonlinear equilibrium relationship that depends on second-order reaction kinetics. A computational approach was devised to solve the Thomas model. The Thomas model's validity was established by conducting three distinct sets of experiments. The first entails the adsorption of acetic acid from the air through the utilization of activated carbon. Following this, zeolite-5A adsorbs trichloroethylene (TCE) from the air. Finally, activated carbon is employed for the purpose of adsorbing o-cresol from aqueous solutions. A study was done to estimate phase equilibria and interphase mass transfer rates. To find the kinetic mass-transfer coefficient (K) for gases, the phase coefficients for mass transfer in the fluid phase (K_f) and the pore phase (K_p) were added together. The estimation of (K) for liquid was performed using the mass transfer coefficient (k_s) for the solid phase and (k_f) togaher. The results suggest that the adsorption of acetic acid from air on activated carbon gives a good agreement with the Thomas model. The other sets of data demonstrate a disparity due to the underlying assumptions inherent in the Thomas model.

Keywords: Adsorption, Fixed bed, Ion exchange, Thomas, Sorption processes

حركية عملية الامتصاص للطبقة الثابتة

ياسمين عبد العزيز مصطفى

قسم اقتصاديات النفط والغاز ، جامعة الامام جعفر الصادق، بغداد، العراق

الخلاصة

إن عمليات الامتزاز والتبادل الأيوني للطور الثابت تكون متغيرة مع الزمن فالمعادلات الخاصة بالتصاميم هي معادلات تفاضلية تحتاج الى حلول بالطرق العددية. توماس استطاع ان يعطي حل عام تحليلي لمعادلات الامتزاز والتبادل الأيوني مستندا على علاقات التوازن الغير خطية وعلى ديناميكية التفاعل من الدرجة الثانية. لقد تم تصميم برنامج على الحاسوب لحل هذه المعادلات حسب موديل توماس. تم استخدام ثلاثة نماذج من التجارب وطبق عليها هذا الموديل، التجربة الأولى حول امتزاز حامض الخليك من الهواء بواسطة الفحم المنشط ، التجربة الثانية حول امتزاز ثلاثي كلورو الإثيلين من الهواء بواسطة الزيولايت، التجربة الثالثة حول امتزاز مادة الاورثوكريسول من الماء بواسطة الفحم المنشط . معاملات التوازن وانتقال الكتلة في الطور البيني تم حسابها. معامل انتقال الكتلة الحركيK للغازات تم حسابه باستخدام معامل انتقال الكتلة خلال السائلK_f ومعامل النتقال الكتلة خلال المساماتK_p. اما للسوائل فان معامل انتقال الكتلة الحركي تم حسابه باستخدام معامل انتقال الكتلة خلال المادة الصلبة K_s و معامل انتقال الكتلة خلال السائل K_f. النتائج بينت ان النموذج الاول اعطى انطباقا جيدا لموديل ثوماس اما النموذج الثاني والثالث حصل بعض الانحراف عن موديل ثوماس بسبب الفرضيات المستعملة في الموديل.

الكلمات المفتاحية : الامتزاز ، التبادل الايوني، الطبقة الثابتة، ثوماس، عمليات الامتصاص.

1. INTRODUCTION

Adsorption is a process in which molecules in a mixture of gases or a liquid solution stick to the surface of a porous solid adsorbent. The adsorbent has the potential to be derived from either natural or synthetic sources. The utilization of adsorption is wide-ranging and encompasses diverse purification methodologies and the retrieval of vital constituents. Different studies **(Salman et al., 2014; Hong et al., 2017; Çermikli et al., 2020; Zhao et al., 2021; Chen and Lo, 2022; Mohamed et al., 2023)** show that molecular sieves and activated carbon have been used a lot to treat solutions.

Batch, fixed bed, fluidized bed, moving bed, and pulsed bed are different process topologies commonly utilized in adsorption systems. Each of these approaches exhibits both advantages and disadvantages. **(Patel, 2019)** asserts that fixed bed columns are extensively employed within the industrial sector to effectively remove various impurities from wastewater.

Within the fixed bed column process framework, it is feasible to generate a graphical depiction illustrating the effluent concentration in relation to time. The term frequently used to describe this visual depiction is a breakthrough curve or concentration history. The mass transfer zone (MTZ) is an area inside the column where the concentration changes from around 90% to 5% of its initial magnitude **(Qian, 2018).** Most of the mass transfer takes place within this specific region. The primary mass transfer zone (MTZ) moves vertically inside the column until it reaches the endpoint in the column; at that point, which is called

the breakthrough point, the adsorbate can be distinguished. Then, the effluent concentration from the column kept increasing until it reached a state of equilibrium where no more adsorptions could be done. The shape and extent of the mass transfer zone (MTZ) are key factors that primarily impact the efficacy of the adsorption column. This region possesses notable practical importance, as it facilitates the derivation and computation of the concentration history **(Patel, 2019)**.

Mass transfer resistance in fixed bed columns is measured by three main factors: external film resistance, intraparticle diffusion resistance, and axial dispersion **(Yao and Chen, 2017; Gadooa and Abbas, 2021)**. To comprehend the sorption process mechanism, it is imperative to possess a thorough understanding of the phenomenological mathematical models utilized in fixed bed processes. The mass transfer in the sorption process is very complicated, especially when the equilibrium isotherms are not linear. The effluent concentration displays both spatial and temporal fluctuations. In such cases, the most suitable mathematical framework for elucidating this phenomenon is a collection of partial differential equations, commonly called the phenomenological model. Nevertheless, the analytical solution to these equations presents considerable difficulties. Due to the complex nature of the subject matter, it is often necessary to make several simplifications in phenomenological mathematical models to obtain a good analytical solution.

Many mathematical models have been developed to predict breakthrough curves in adsorption procedures involving fixed beds. Several models frequently employed in the field encompass the Thomas, Adams, and Bohart models, the bed depth service time model, Yoon-Nelson and Clark models. The Thomas model has been widely utilized among the examined models, as noted by many authors (**Petal, 2019; Amiri et al., 2019; Omitola et al., 2022).** This specific model forecasts the sorption process, assuming that internal and external diffusion resistances can be neglected. The elucidation of the sorption process can be achieved by employing pseudo-second-order reversible reaction kinetics, and the quantification of the sorption rate may be efficiently accomplished by utilizing the Langmuir adsorption model at equilibrium.

The sorption process observed in a fixed bed can be described as an unsteady rate-controlled process, as indicated by the researcher **(Amiri et al., 2019; Feizi et al., 2021)**. The interdependence of time and position influences the concentrations in both the fluid and solid phases inside the bed. The differential equations that control the design of unsteady-state sorption processes require numerical methods for their solution. The current analytical solution, as suggested by **(Thomas, 1944)**, incorporates second-order reaction kinetics and can also be applied to systems with diffusion limitations.

The primary aim of this work is to showcase the predictive capacity of the Thomas model in determining the breakthrough curves for ion exchange and adsorption. The objective will be accomplished by employing three separate datasets encompassing gaseous and liquid phases. The original experiments focused on the adsorption of acetic acid from air using activated carbon. The subsequent set investigated the adsorption of trichloroethylene (TCE) from the air using zeolite-5A. Finally, the third set of studies investigated the adsorption process of O-cresol from water using activated carbon. A computational technique addressed the mathematical model by incorporating all the requisite equations and constants.

2. THEORY

2.1 Method of Second-Order Kinetics

The reaction type for ion exchange and physical adsorption can be shown **(Mustafa and Ebrahim, 2010)**:

A+ B. Resin →B+A. resin (ion exchange)   (1)

A+ Sorbent → A. Sorbent (adsorption)   (2)

The rate for ion exchange at the particle surfaces, in the case of ions of the same valence, may be expressed as:

$$\frac{d(A.Resin)}{dt} = K_{kin}\left[(A)(B.Resin) - \left(\frac{1}{k}\right)(B)(A.Resin)\right]$$ (3)

Parentheses indicate the concentration, whereas the variable t denotes time. The symbol K_{kin} represents the rate factor associated with the reaction, while the symbol k denotes the equilibrium constant of the reaction. Given that the resin possesses a limited capacity, it follows that the total concentrations of $(B.Resin)$ and $(A.Resin)$ are equivalent to a constant value.

$$(B.Resin) + (A.Resin) = \bar{Q}$$ (4)

Likewise, during the solution phase external to the resin, the total concentrations of species A and B remain constant.

$$(A) + (B) = (C_0)$$ (5)

The following substitutions may then be made:

$$(A) = (C)$$ (6)

$$(B) = (C_0 - C)$$ (7)

$$(A.Resin) = (q)$$ (8)

$$(B.Resin) = (\bar{Q} - q) = (q_\infty - q)$$ (9)

The variable q represents the quantity of A in gram-equivalents per unit weight of dry resin. $\bar{Q}$ represents the maximum capacity of the dry adsorbent, measured in gram-equivalents per unit weight. q_∞ represents the capacity of the adsorbent when it reaches saturation. In the context of ion exchange, $q_\infty = \bar{Q}$. Consequently, Eq. (3) can be expressed as:

$$\left(\frac{dq}{dt}\right) = K_{kin}\left[C(q_\infty - q) - \frac{1}{k}q(C_0 - C)\right]$$ (10)

The rate of adsorption at the solid surfaces assuming "Langmuir" equilibrium under isothermal reaction may be written **(Mustafa and Ebrahim, 2010):**

$$\frac{d(A.Sorbent)}{dt} = K_{kin}\left[(A)(Sorbent) - \frac{1}{k}(A.Sorbent)\right]$$ (11)

then let $(A) = (C)$ (12)

$$(A.Sorbent) = (q) \tag{13}$$

$$(Sorbent) = (\bar{Q} - q) \tag{14}$$

$$\left(\frac{dq}{dt}\right) = K_{kin}\left[C(\bar{Q}-q) - \frac{1}{K_{ads}}q\right] \tag{15}$$

2.2 EQUATIONS of TRANSPORT

The material balance on the fluid and solid phases for an infinitesimal thickness of bed at any given cross-section is expressed as **(Gadooa and Abbas, 2021)**:

$$\varepsilon\frac{\partial C}{\partial t} + \rho_B\frac{\partial q}{\partial t} + U\frac{\partial C}{\partial Z} = D_L\frac{\partial^2 C}{\partial^2 Z} \tag{16}$$

D_L is the axial dispersion coefficient. To eliminate the effect of axial dispersion, $D_L the$ term is set to zero then **(Chu, 2010)**:

$$\varepsilon\frac{\partial C}{\partial t} + \rho_B\frac{\partial q}{\partial t} + U\frac{\partial C}{\partial Z} = 0 \tag{17}$$

Eq. 17 must be coupled with another equation representing the behavior of the solid phase:

$$\rho_B\frac{\partial q}{\partial t} = Ka\, F(C,q) \tag{18}$$

Using the interphase mass-transfer coefficient, Ka, and a driving force, $F(C,q)$, this equation shows how to measure the rate at which solute is added to the solid phase. Solving these two equations is important in fixed-bed column design for sorption and ion exchange processes.

3. THOMAS SOLUTION for SORPTION BREAKTHROUGH CURVES

Thomas offers the most comprehensive and insightful analysis of the sorption design challenge. The Thomas model, as initially introduced by **(Thomas, 1944)**, integrates the Langmuir isotherm and pseudo-second-order kinetics while neglecting the influence of axial dispersion inside the adsorption column **(Feizi et al., 2021; Dadebo et al., 2023).**
Thomas postulated that the rate of adsorption in Eq. (18) can be described by:

$$\rho_B\frac{\partial q}{\partial t} = Ka\left[c\left(1-\frac{q}{q_m}\right) - \frac{1}{k}(C_o - C)\frac{q}{q_m}\right] \tag{19}$$

The term included between square brackets is commonly referred to as the kinetic driving force, while the accompanying kinetic coefficient is denoted by the symbol k. Eq. (19) is simplified for subsequent use by changing the temporal scale.

$$\theta = t - \frac{\varepsilon Z}{U} \tag{20}$$

Then Eq.s (17, 19) becomes:

$$\rho_B\frac{\partial q}{\partial \theta} + U\frac{\partial C}{\partial Z} = 0 \tag{21}$$

$$\rho_B \frac{\partial q}{\partial \theta} = Ka \left[C \left(1 - \frac{q}{q_m} \right) - \frac{1}{k} \frac{q}{q_m} (C_o - C) \right] \tag{22}$$

Thomas successfully transformed the dependent variables to reduce Eqs. (21 and 22) to a linear equation. The proposed approach for addressing adsorption boundary conditions at Z and θ involves setting the concentration C (0, θ) = C_o = constant at Z=0 and the capacity q (Z, 0) = 0 at $\theta = 0$. Then the solution can be shown (**Chu, 2010)** as:

$$X = \frac{J(\bar{R}N, N\bar{T})}{J(\bar{R}N, N\bar{T}) + (1 - J(N, \bar{R}N\bar{T})) \exp((\bar{R}-1)N(\bar{T}-1)} \tag{23}$$

where:

$$J(u, v) = 1 - \emptyset_1(u, v) \tag{24}$$

$$\emptyset_1(u, v) = \int_0^u \emptyset_0(\lambda, v) \, d\lambda \tag{25}$$

$$\emptyset_0(\lambda, v) = exp(-\lambda - v) I_o(2\sqrt{\lambda}v \tag{26}$$

where I_o is the modified Bessel function of zero order. The approximate calculation of the J function is:

$$J(u, v) = \frac{1}{2} \left[1 - erf \left(\sqrt{u} - \sqrt{v} + \frac{exp\left[-(\sqrt{u}-\sqrt{v})^2\right]}{\sqrt{\pi}\left[\sqrt{v} + (uv)^{1/4}\right]} \right) \right] \tag{27}$$

Eq. (23) of the breakthrough curve was adapted to a revised format that is appropriate for implementation on microcomputers **(Tan, 1984; Mustafa and Ebrahim, 2011)** by:

$$\frac{1}{x} = 1 + \exp(G) \tag{28}$$

$$G = In[\emptyset_1(N, \bar{R}N\bar{T})] - In[J(\bar{R}N, N\bar{T})] + (\bar{R}-1)N(\bar{T}-) \tag{29}$$

$$\emptyset_1(N, \bar{R}N\bar{T}) = J(\bar{R}N\bar{T}, N)[1 - \emptyset_0(\bar{R}N\bar{T}, N) / J(\bar{R}N\bar{T}, N) \tag{30}$$

$$\emptyset_0(u, v) = \frac{exp\left[-(\sqrt{u}-\sqrt{v})^2\right]}{2\sqrt{\pi}(u*v)^{1/4}} \tag{31}$$

The integral error function, erf, was approximated as follows **(Forbes and Underhill, 1986)**.

$$erf x = 1 - (a_1 t + a_2 t^2 + a_3 t^3 + a_4 t^4 + a_5 t^5) e^{-x^2} \tag{32}$$

where t= $\frac{1}{1+BX}$ \hfill (33)

a_1=0.254829592 ; a_2=-0.284496736 ; a_3=1.421413741; a_4 =-1.453152027
a_5=1.061405429 ; B=0.3275911

The number of transfer units N, the separation factor $\bar{R}$ and the throughput parameter $\bar{T}$ can be calculated as follows **(Perry and Chilton, 1973):**

$$N = \frac{KaZ}{U} \tag{34}$$

$$\bar{R} = \frac{1}{\bar{\bar{k}}} \tag{35}$$

$$\bar{T} = \frac{U C_o\, \theta}{q_m\, Z \rho_b} \tag{36}$$

$$\theta = t - \frac{\varepsilon Z}{U} \tag{37}$$

A program flow chart, depicted in **Fig. 1**, was utilized to build a computer program to calculate the outlet concentration at any given time and generate a breakthrough curve. The program was employed to compute the values of , K_p, K_f, K, N and $\bar{R}$ Subsequently, for each time interval $\bar{T}$, the concentration at outlet C, was determined. The equations employed for estimating the kinetic coefficient, denoted as K, in the Thomas formula for gas sorption were derived from the work of **(Perry and Chilton, 1973)**.

$$D_f = D_0 \left(\frac{T}{T_0}\right)^2 \frac{P_0}{p} \tag{38}$$

$$D_k = \frac{19400x}{S_g\, \rho_\rho} \sqrt{\frac{T}{M}} \tag{39}$$

$$\frac{1}{D_p} = \frac{\tau}{x}\left(\frac{1}{D_k} + \frac{1}{D_f}\right) \tag{40}$$

$$k_p = \frac{60 D_P}{s_0 (1-\varepsilon)\, d_p^2} \tag{41}$$

$$\text{where } S_0 = \frac{particle\ external\ area}{volume\ of\ particle} \tag{42}$$

$$k_f = \frac{J_D U}{(SC)^{2/3}} \tag{43}$$

$$\text{where } J_D = 1.175(Re)^{-0.415} \tag{44}$$

$$\text{then } \quad \frac{1}{K} = \frac{\bar{\bar{K}}+1}{2\bar{\bar{K}}}\left(\frac{1}{K_p} + \frac{1}{K_f}\right) \tag{45}$$

where

$$\bar{\bar{k}} = 1 + \bar{k}p \tag{46}$$

$$and\ p = \frac{RT C_0}{M} \tag{47}$$

and k can be estimated for liquid sorption as follows:

$$\frac{1}{K} = \frac{\bar{\bar{k}}+1}{2\bar{\bar{k}}}\left(\frac{C_0/q_m\, \rho_b}{k_s} + \frac{1}{k_f}\right) \tag{48}$$

$$\text{where } \bar{\bar{k}} = 1 + \bar{k}C_o \tag{49}$$

$$k_s = \frac{15 D_S}{(1-\varepsilon) d_p} \tag{50}$$

The surface diffusion coefficient D_S can be estimated following the procedure adopted by **(Carman and Haul, 1954).**
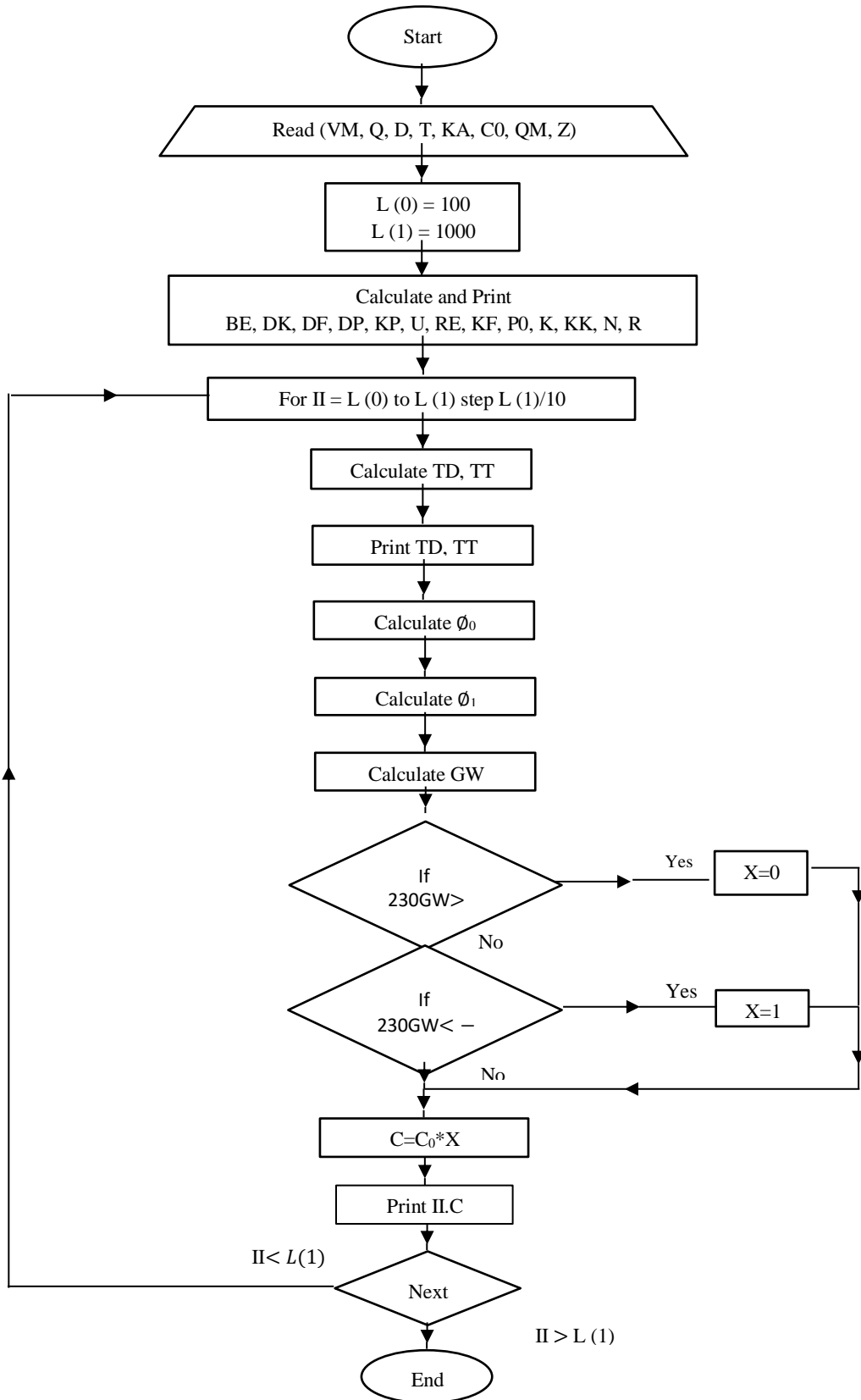
Figure 1. Program Flow chart.

K_f Can be estimated from the semi-empirical correlation **(Perry and Chilton, 1973)**.

$$K_f = \frac{D_0}{d_e} \left[2 + 1.45(R_e)^{1/2} \, (S_C)^{1/3} \right] \tag{51}$$

where d_e is the equivalent diameter for a non-spherical particle of adsorbent, which can be calculated as follows:

$$d_e = \frac{4\varepsilon}{(1-\varepsilon)S_0} \tag{52}$$

4. RESULTS AND DISCUSSION

Three sets of experiments **(Maghazachi, 1989; Ibrahim, 1992; Mustafa, 1992)** are employed and compared with the theoretical frameworks put forward by Thomas et al. **Table 1** displays the system characteristics that were employed in the assessment of resistances. The first work examines the mechanism of acetic acid adsorption from the air using activated carbon.

Table 1. Values of system parameters used for estimating resistance

Symbol	Units	1st Set	2nd Set	3rd Set
ρ_b	g/cm³	0.4	0.715	0.4
ρ_p	g/cm³	1.4	1.044	1.4
d_p	cm	0.068x0.26	0.235	0.068x0.26
T	K	303	305	313
D_0	cm²/sec	0.1064	0.065	1.33×10^{-5}
D_k	cm²/sec	2.56×10^{-3}	3.30×10^{-3}	-
D_p	cm²/sec	3.28×10^{-3}	6.58×10^{-4}	-
D_s	cm²/sec	-	-	0.6×10^{-7}
K_p	cm/sec	2.53	0.04	-
K_s	cm/sec	-	-	4.63×10^{-5}
Re	-	61.5	4.73	12.87
Sc	-	1.16	1.40	4962
K_f	cm/sec	30	1.19	2.34×10^{-3}
K	cm/sec	4.29	5.9×10^{-2}	4.07×10^{-3}
Q	cm³/sec	277.8	4.66	0.75
U	cm/sec	157.2	2.32	0.4
C_0	g/cm³	43.743×10^{-6}	578×10^{-6}	100×10^{-6}
Z	cm	20	17.5	6
N	-	9	7.8	1
$\overline{R}$	-	0.088	0.334	0.45
$\overline{T}$	-	0.176	0.265	0.131
ε	-	0.714	0.315	0.715
q_m	g/g	0.4876	0.0446	0.271

The second set investigates the adsorption process of trichloroethylene (TCE) from the air by utilizing zeolite-5A. The third study examines the adsorption process of O-cresol from water using activated carbon.

Figs. 2 to 4 illustrate the plotted breakthrough curves for the experimental and theoretical data. **Fig. 2** shows a comparative study conducted between the Thomas model and the experimental data pertaining to the first data set. The average absolute error, which was 6%, demonstrates significant agreement. **(Chu, 2010)** asserts that the Thomas model has demonstrated reliable and accurate results. However, it requires a detailed representation of its analytical formulation. The research by **(Vilvanathan and Shanthakumar, 2017)** shows that the Thomas model is a good way to describe the adsorption kinetics and designing fixed bed adsorption columns, especially within a noticeable range of flow rates and bed heights. In their research study, **(Dadebo et al., 2023)** used the Thomas model to predict the empirical data for the fixed bed adsorption column. Significantly, the findings of their inquiry produced positive outcomes.
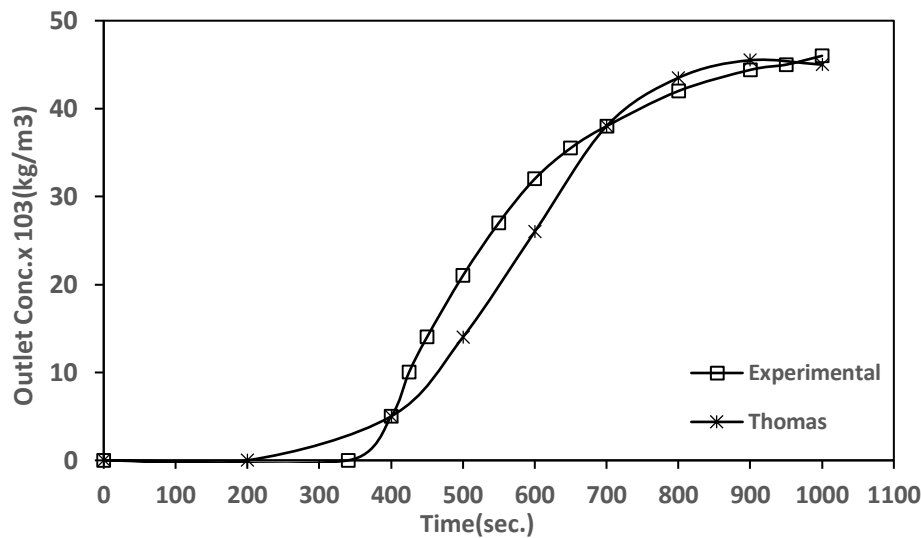
Figure 2. Experimental and predicted breakthrough behavior for adsorption of acetic acid from air by activated carbon
($Q=2.778 \times 10^{-4}$ m^3/sec., $C_o=43.743 \times 10^{-3}$ kg/m^3, T= 303 K, Z=20 $\times 10^{-2}$ m).

Fig. 3 illustrates a comprehensive comparison between the empirical and theoretical data related to the second dataset. The Thomas model exhibits a significant connection with the empirical findings, particularly when analyzing time values beyond t = 400 seconds. However, a greater range of values is observed below this threshold because of the implementation of low velocity and high concentration in the respective experiments, as evidenced in **Table 1**. In this specific context, it is imperative to consider the presence of axial dispersion inside the resin particle. The axial dispersion phenomenon becomes notable in porous particles when subjected to low flow rates and quick, intensive sorption, particularly in gases characterized by low Reynolds numbers.

(Cen and Yang, 1986) established a temporal solution for the breakthrough curves of zeolite adsorbers. The proposed approach encompasses three distinct stages of diffusion, specifically the external film, macropore, and micropore phases, which are mathematically represented as an infinite series. The expected breakthrough curve that **(Cen and Yang, 1986)** produced provided a dependable representation of the empirical data obtained for set 2, which relates to the adsorption of trichloroethylene (TCE) from the air using Zeolite-5A as shown in **Fig. 3**. The average absolute error of 6% was obtained, as reported by **(Ibrahim, 1992)**.
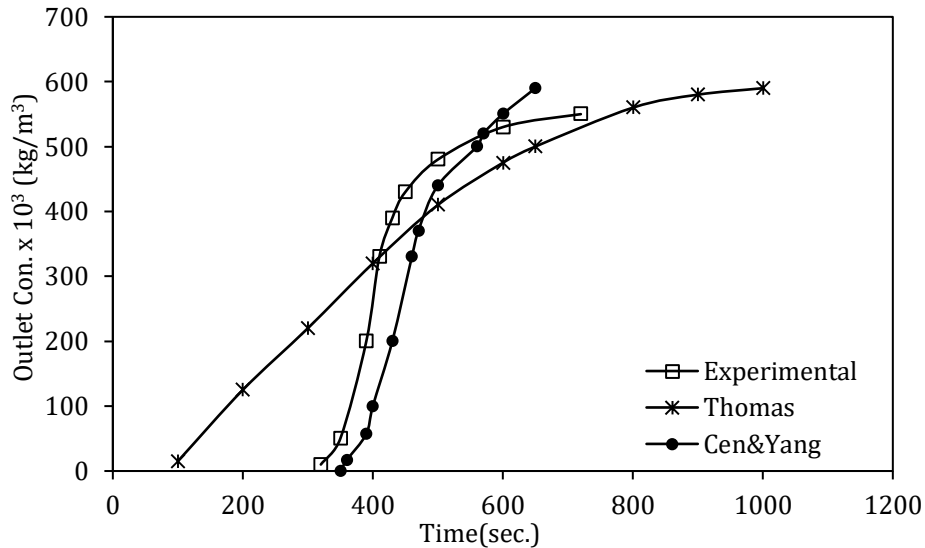
Figure 3. Experimental and predicted breakthrough behavior for adsorption
of TCE from Air by zoolite 5A
(Q=4.66×10⁻⁶ m³/sec., C₀=0.578 kg/m³, T=305 K, Z=17.5×10⁻²m).

Fig. 4 illustrates a comparative study conducted between the Thomas model and empirical findings for the third dataset. The observed deviation between the Thomas model and the experimental curve can be ascribed to the application of a singular value for the number of transfer units (N = 1) in the specific dataset, as presented in **Table 1**. **(Chu, 2010)** posits that an increased quantity of transfer units (N≥10) is linked to a diminished degree of deviation. (**Liaw et al., 1979)** did a successful study that found a way to describe the kinetics of a fixed bed adsorber. The solution includes both external and intraparticle diffusion. The concordance between the anticipated breakthrough curve and the empirical observations was deemed acceptable, as illustrated in **Fig. 4**. As to the findings of **(Mustafa, 1992)**, the average absolute error was established at 4%.
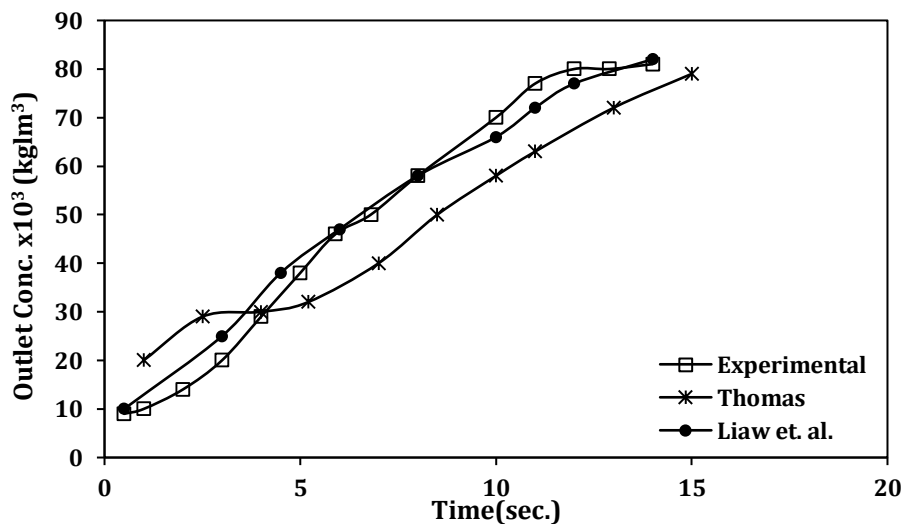
Figure 4. Experimental and predicted breakthrough curves for adsorption of O-Cresol
from water by activated carbon
(Q=7.5×10⁻⁷ m³/sec., C₀=100×10⁻³ kg/m³, T=313K, Z=6×10⁻²m)

5. CONCLUSIONS

The Thomas model is a frequently utilized theoretical framework for forecasting breakthrough curves in fixed bed systems that encompasses the analysis of adsorption and ion exchange phenomena in both gaseous and liquid phases. The efficacy of the Thomas model in accurately forecasting the sorption breakthrough curve was proven by conducting three separate experimental trials. The model was employed to calculate the phase equilibria and rates of mass transfer between phases. The phase coefficients K_f, and K_p were combined to determine the kinetic mass-transfer coefficients K for gases and K_f and K_s for liquids. Thomas proposed a thorough methodology that considers the non-linear nature of equilibrium connections.

The first set of experiments revealed a notable level of agreement between the Thomas model and the empirical data, as evidenced by an average absolute variation of 6%. The second dataset demonstrates a variation in the early stages of the experiment, which can be attributed to the presence of low velocity and high concentration. One possible explanation for this phenomenon may be the exclusion of axial dispersion in the Thomas model. The observed mismatch in the third model can be attributed to the existence of one mass transfer unit within the column. The first dataset demonstrates that greater mass transfer units yield more favorable results.

NOMENCLATURE

a	Interfacial area of solid phase per volume of bed (cm^2/cm^3)	$\bar{Q}$	The ultimate capacity of the dry adsorbent (g/g)
b	Coefficient of Langmuir equation ($\frac{1}{Pa}$ or $\frac{cm^3}{g}$)	Q	Volumetric flow rate (cm^3/sec)
C	Concentration of fluid (kg/m^3)	q	Adsorbed phase concentration (capacity) (g/g)
C_o	Initial concentration (kg/m^3)	q_m	Maximum solid phase concentration value corresponding to complete coverage of the surface by a monolayer (g/g)
D_0	Molecular diffusivity (cm^2/sec)	q_∞	Adsorped phase concentration at saturation (g/g)
D_f	Fluid phase diffusivity (cm^2/sec)	R	Gas constant = 8.3143 kJ/kmol k
D_k	Knudsen diffusion coefficient (cm^2/sec)	$\bar{R}$	Separation factor
D_L	Axial desperation coefficient (cm^2/sec)	S_0	External surface area per unit volume of a particle 1/cm
D_p	Particle phase diffusivity (cm^2/sec)	T	Temperature (K)
D_S	Surface diffusivity (cm^2/sec)	$\bar{T}$	Throughput parameter
d_e	The equivalent diameter of the particle (cm)	t	Time (sec)
d_p	Diameter of the particle (cm)	U	Superficial fluid velocity (cm/sec)

k_f	Mass transfer coefficient for fluid phase (cm/sec)	X	C/Co normalized concentration
k_p	Mass transfer coefficient in pore phase (cm/sec)	Z	Bed height (cm)
k_s	Mass transfer coefficient for solid phase (cm/sec)	θ	Contact time (sec)
K	Kinetic mass transfer coefficient for Thomas formula (cm/sec)	ρ_b	Bulk density of bed (g/cm^3)
$\bar{k}$	Equilibrium constant or Langmuir constant (cm^3/g)	ρ_p	Particle density (g/cm^3)
M	Molecular weight (g/mol)	τ	Tortuosity factor
N	Number of transfer units	x	Fraction void space inside the porous particles
P	Adsorbate partial pressure (K. Pa)	R_e	Reynolds number
		S_c	Schmidt number

REFERENCES

Amiri, M.J., Khozaei, M., and Gil, A., 2019. Modification of the Thomas model for predicting unsymmetrical breakthrough curves using an adaptive neural-based fuzzy inference system, *J Water Health*, 17 (1), pp. 25–36. Doi:10.2166/wh.2019.210.

Carman, P.C., and Haul, R.A.W., 1954. Measurement of diffusion coefficients, Proceedings of the Royal Society, 222, pp. 109-117. Doi:10.1098/rspa.1954.0056.

Cen, P.L., and Yang, R.T., 1986. Analytic solution for adsorber breakthrough curves with bidisperse sorbents (zeolites), American Institute of Chemical Engineering, 32(10), P. 1635. Doi:10.1002/aic.690321007.

Çermikli, E., Şen, F., Altıok, E., Wolska, G., Cyganowski, P., Kabay, N., Bryjak, M., Arda, M., Yüksel, M., 2020. Performances of novel chelating ion exchange resins for boron and arsenic removal from saline geothermal water using adsorption-membrane filtration hybrid process, Desalination, 491. P.114504. Doi:10.1016/j.desal.2020.114504.

Chen, H.Y. and Lo, I.T., 2022. Theoretical and Experimental Adsorption of Silica Gel and Activated Carbon onto Chlorinated Organic Compounds in Water: A Case Study on the Remediation Assessment of a Contaminated Groundwater Site. *Applied Sciences*, *12*(23), P.11955. Doi:10.3390/app122311955.

Chu, K.H., 2010. Fixed bed sorption: setting the record straight on the Bohart-Adams and Thomas models. *J. Hazardous Materials*, 177 (1–3), pp. 1006–1012. Doi:10.1016/ j. jhazmat.2010.01.019.

Dadebo, D., Atukunda, A., Ibrahim, m.G., Nasr, m., 2023. Integrating chemical coagulation with fixed-bed column adsorption using rice husk-derived biochar for shipboard bilgewater treatment: Scale-up design and cost estimation, *Chemical Engineering Journal Advances*, P.100520. Doi:10.1016/j.ceja.2023.100520.

Feizi, F., Sarmah, A.K., and Rangsivek, R*.,* 2021. Adsorption of pharmaceuticals in a fixed-bed column using tyre-based activated carbon: Experimental investigations and numerical modeling. *Journal of Hazardous Materials*, 417, P. 126010. Doi:10.1016/j.jhazmat.2021.126010.

Forbes, S.L., and Underhill, D.W., 1986. Modeling adsorption bed behavior using microcomputer. *Air Pollution Control Association*, 36(1), P. 61. Doi: 10.1080/00022470.1986.10466047.

Gadooa, Z.A., and Abbas, M.N., 2021. Mathematical Modelling Of Heavy Metals Removal From Petroleum Refinery Wastewater. *Journal of Engineering and Sustainable Development (JEASD)*, *25* (Special_ Issue_2021). Doi:10.31272/jeasd.conf.2.3.3.

Hong, S., Hangxi, L., Ping, A., Lin, H., Xingang, Li, and Shan Cong, 2017. Application of silica gel in removing high concentrations toluene vapor by adsorption and desorption process *Journal of the Taiwan Institute of Chemical Engineers*, 74, pp. 218-224. Doi:10.1016/j.jtice.2017.02.019

Ibrahim, S.K., 1992, Removal of gaseous pollutants from air by adsorption method, M.Sc. Thesis, University of Baghdad.

Liaw, C.H., Wang, J.S.P., GreenKorn, R.A. and Chao, K.C., 1979. Kinetics of fixed-bed adsorption: a new solution, *American Institute of Chemical Engineering*, 25(2), P. 376. Doi:10.1002/aic.690250229.

Maghazachi, M.S.K., 1989. Removal of gaseous pollutants from air by adsorption method, M.Sc. Thesis, University of Baghdad.

Mohamed, E.F., El-Mekawy, A., Ahmed, S.A.S. and Fathy, N.A., 2023. High Adsorption Capacity of Ammonia Gas Pollutant Using Adsorbents of Carbon Composites. *Arabian Journal for Science and Engineering*, pp. 1-11. Doi:10.1007/s13369-023-07987-3.

Mustafa Y.A., 1992. Removal of pollutants from water by adsorption, M.Sc. thesis, University of Baghdad.

Mustafa, Y.A., and Ebrahim, S.E., 2010. Utilization of Thomas model to predict the breakthrough curves for adsorption and ion exchange, *Journal of Engineering,* 16(4), pp. 6206 -6223.

Omitola, O.B., Abonyi, M.N., Akpomie, K.G., and Dawodu, F.A., 2022. Adams-Bohart, Yoon-Nelson, and Thomas modeling of the fix-bed continuous column adsorption of amoxicillin onto silver nanoparticle-maize leaf composite. *Applied Water Science*. 12(5), P. 94. Doi:10.1007/s13201-022-01624-4.

Patel, H., 2019. Fixed-bed column adsorption study: a comprehensive review, *Applied Water Science*, 9(3). Doi:10.1007/s13201-019-0927-7.

Perry, R. H., and C.H. Chilton, C. H.,1973. Chemical Engineering Handbook, 5th ed., McGraw-Hill.

Qian, W., Song, Q., Ding, H. and Xie, W., 2019. Computational simulations of the mass transfer zone in GS adsorption column packed with Fe^{3+} type ion exchanger. *Chemosphere*, *215*, pp. 507-514. Doi: 10.1016/j.chemosphere.2018.10.054.

Salman, M.S., Abood, W.M. and Ali, D., 2014. Batch and Fixed-Bed Modeling of Adsorption Reactive Remazol Yellow Dye onto Granular Activated Carbon. *Journal of Engineering*, *20*(8), pp. 156-176. Doi:10.31026/j.eng.2014.08.10

Tan, H.S., 1984. *Programs for fixed-bed sorption*. Chemical engineering (New York, NY), 91(26), pp. 57-61.

Thomas, H.C., 1944. Heterogeneous ion exchange in a flowing system, *Journal of the American Chemical Society*, 66, pp. 1664-1666. Doi:10.1021/ja01238a017.

Yao, C., Chen, T., 2017. A film-diffusion-based adsorption kinetic equation and its application. *Chemical Engineering Research and Design*, pp. 87-92. Doi:10.1016/j.cherd.2017.01.004.

Vilvanathan, S. and Shanthakumar, S., 2017. Column adsorption studies on nickel and cobalt removal from aqueous solution using native and biochar form of Tectona grandis. *Environmental Progress & Sustainable Energy*, 36(4), pp. 1030–1038. Doi:10.1002/ep.12567.

Zhao, X., Feng, T., Wang, P. and Liao, Z., 2021. Study on the effect of soft and hard coal pore structure on gas adsorption characteristics. *Advances in Civil Engineering*, *2021*, pp. 1-10. Doi:10.1155/2021/1425227.

APPENDIX

List of Computer Program

```
10 DIM C (1000), YI (1000)
20 L (0) = 100: L (1) =1000
30 REM .
40 REM --------------------------------
50 DATA 0.152, 277.8, 1.5, 303, 5.6479, .000043743, .4876, 20
60 KI=.784: DO O =.6: M (1) = 60.5: RB = .4: RP = 1.4: D2 = .068: SG = 9500000!
70 D0 =.1064: D1=.17: S=16.8
80 READ VM, Q, D, T, KA, C0, QM, Z
90 REM------------------------------------
100 BE= 1- (RB / RP): PRINT "BED VOID FRACTION="; BE
110 DK =19400 . KI / (SG* RP): DK= DK* (SQR (T / M (1)) )
120 PRINT "DK"; DK; "CM ^2/SEC"
130 DF ((T/ 273) ^ 2)* DO
140 PRINT "DE"; DF; "CM^ 2/SEC"
150 DP =1 / DK + 1 / DE: DP =KI / (DOO* DP)
160 PRINT "DP="; DP; "CM^2/SEC"
170 KP= 15* DP / D2 *(1- BE))
180 PRENT"KP="; KP; "CM/SEC"
190 SC =VM /DF: UF =4* Q / (3.141593*D^2)
200 RE =UF/ (VM*SO)
210 PRENT" U="; UF; "CM/SEC"; "&";"RE="; RE
220 GD = 1.17 * (RE ^ (-.415))
230 KF = UF. JD / (SC ^ (2 / 3))
240 PRENT" KF ="; KF; "CM /SEC"
250 PO = 8.314 *T *C0 / M (1): P0 =P0* 1000
260 K =1 + KA * P0
270 PRINT "P0="; P0;" KPa ";" & "; "K="; K
280 KK = (K + 1) * (1/ KP + 1 / KF) / (2 *K)
290 KK = 1 / KK: PRINT "MASS TRANSFER COEFFICIENT KK="; KK; "CM/SEC."
300 PRINT" A="; KK* SO; "1/SEC".
310 PRINT
320 N= KK* SO* Z / UF: PRINT "N"; N
330 R=1/K: PRINT "R="; R
340 PRINT: CA= 0
350 REM * THE J FUNCTION CALCULATION*
360 REM-------------------------------------------
370 FOR II= L (0) TO L (1) STEP L (1)/ 10
380 CA =1+ CA: TI = II: YI (CA) =TI
390 PRINT" LOOP NO."; CA: PRINT
400 TD= TI- Z* BE/UF: PRINT "CONTACT TIME="; TD; "SEC."
410 TT= UF* C0*TD / (QM* RB* Z): PRINT "T="; TT
420 NT= N*TT: PRINT "NT="; NT
430 U=N *R* TT: V=N: GOSUB 640
440 FI (1) =J
450 U=R*N* TT: V=N *TT: GOSUB 910
460 FO=KH
470 WE=FI (1) * (1÷FO / FI (1))
```

```
480 U=R* N: V=N*TT: GOSUB 640
490 EI (2) = J
500 GW= LOG (WE) - LOG (F1 (2)) ÷ (R-1)* N* (TT- 1)
510 IF GW >230 THEN 620
520 IF GW <-230 THEN 630
530 X=1÷ EXP (GW): x=1 / x
540 REM*** PRINTING THE RESULTS***
550 REM ----------------------------------------
560 C (CA) = X*C0
570 PRINT"T="; II; "SEC."
580 PRINT "C = "; C(CA)∶ "g/cm^3"
585 Input x
590 PRINT
600 NEXT II
610 GO TO 950
620 X = 0: GOTO 550
630 X = 1: GOTO 550
640 REM ** SUB R. [erf. & j FUN.]
650 REM ===================
660 ZZ = 0: ERF = 0: Z1= U * U – V * V
670 REM *** erf ***
680 REM  ---
690 A (1) = .254829592 #
700 A (2) = -.284496736 #
710 A (3) = 1.421413741 #
720 A (4) = - 1.453152027 #
730 A (5) = 1.061405429 #
740 P = .3275911
750 O = 1
760 IF z1 < 0 THEN O = -O
770 zz = ABS (z1):  T = 1 / (1+P * zz)
780 FOR I = 1 TO 5
790 ERF = ERF + A (I) * T * I
800 NEXT I
810 ERF = 1 – ERF * EXP (-1 * z1 ^ 2): ERF = O * ERF
820 REM ------------------------------------
830 REM *** J (u, v) ***
840 REM ------
850 A (1) = EXP (-1 * z1 ^ 2)
860 A (2) = 2 * SQR (3.141592654 #)
870 A (2) = ((V * V) + (V * U) ^ (1 / 4)) * A (2)
880 J = .5 * (1- ERF + (A (1) / A (2)))
890 RETURN
900 REM xxxxxxxxxxxxxxxxxxxxxxxxxxx
910 H1 = (-1) * (((U * U) – (V * V)) ^ 2)
920 H2 = 2 * ((SQR (3.14159265#)) * ((V * U) ^ (1/ 4)))
930 KH = (EXP (H1)) / H2
940 RETURN
950 END
```

Program Excute

BED VOID FRACTION= .7142857	LOOP NO.3
DK= 2.559233E-03 CM^2/SEC	.CONTACT TIME= 299.9091 SEC
DF= .1310695 CM^2/SEC	T= .5286939
DP= 3.280019E-03 CM^2/SEC	NT= 4.849976
KP= 2.532367 CM/SEC	.T= 300 SEC
U= 157.2026 CM/SEC & RE= 61.56118	C= 8.341025E-07 g/cm^3
KF= 30.14315 CM/SEC	LOOP NO.4
P0= 1.821402 KPa & K= 11.2871	.CONTACT TIME= 399.9091 SEC
MASS TRANSFER COEFFICIENT KK= 4.291962 CM/SEC	T= .7049786
	NT= 6.467125
A= 72.10495 1/SEC	.T= 400 SEC
N= 9.173505	C= 3.422138E-06 g/cm^3

R= 8.859674E-02
LOOP NO.1
CONTACT TIME= 99.90913 SEC
T= .1761245
NT= 1.615679
T= 100 SEC
C= 4.434135E-08 g/cm^3
LOOP NO.2
CONTACT TIME= 199.9091 SEC
T= .3524092
NT= 3.232828
.T= 200 SEC
C= 1.938902E-07 g/cm^3

LOOP NO.5
.CONTACT TIME= 499.9091 SEC
T= .8812634
NT= 8.084274
.T= 500 SEC
C= 1.182694E-05 g/cm^3
LOOP NO.6
.CONTACT TIME= 599.9091 SEC
T= 1.057548
NT= 9.701422
.T= 600 SEC
C= 2.703398E-05 g/cm^3